Nepal Journal of Mathematical Sciences (NJMS)
ISSN: 2738-9928 (online), 2738-9812 (print)
Vol. 07, No. 01, 2026 (March): 13-26
DOI: https://doi.org/10.3126/njmathsci.v7i1.92214

Research Article
Received Date:November 3, 2025
Accepted Date:February 15, 2026
Published Date:March 28, 2026

Fractional-Order Derivative Model for COVID-19 Transmission Dynamics in Nepal

Hem Raj Pandey

School of Engineering, Faculty of Science and Technology, Pokhara University, Nepal

Corresponding Author: hpandey@pu.edu.np

Abstract: *This study proposed a fractional-order SVEIDR model to investigate the transmission dynamics of COVID-19 in Nepal. By incorporating a fractional derivative of order η, the model captures memory effects such as waning vaccine-induced immunity and behavioral responses that are not adequately represented in classical integer-order frameworks. The establishment of the positivity and boundedness for the solutions, which ensured that the model is well-posed and that the feasible region is closed and bounded within the biologically meaningful domain. The basic reproduction number R_0 is derived using the next-generation matrix method, providing a threshold parameter that governs disease persistence or eradication. Numerical simulations calibrated with Nepal-specific COVID-19 data demonstrate the influence of vaccination coverage and the fractional order η on the epidemic model. The results concluded that fractional-order dynamics yield improved agreement with observed data compared to classical integer-order models, particularly in capturing the memory-driven effects of vaccination intervention responses. The proposed model offers both theoretical insights and appropriate guidance for the transmission dynamics of COVID-19 in Nepal.*

Keywords: COVID-19 disease, Caputo's fractional derivative, Basic reproduction number, Fractional Euler's method, Graphical simulations.

1 Introduction

The emergence of coronavirus disease in the year 2019 (COVID-19), caused by the novel severe acute respiratory syndrome coronavirus-2 (SARS-CoV-2), has significantly disrupted health systems, economies, and societies across the globe [4]. Since its identification in late 2019, the pandemic has spread rapidly, leading to multiple waves of infection and immense public health challenges. Nepal confirmed its first COVID-19 case in January 2020. In the years that followed, the country experienced multiple waves of the pandemic, most notably the Delta surge in mid-2021 and the Omicron surge in early 2022. By 2025, Nepal had recorded approximately 1,003,450 infections, with 12,031 deaths and 991,322 recoveries[22]. The relatively limited healthcare infrastructure, combined with heterogeneous vaccination coverage and varying adherence to public health measures, has made Nepal particularly vulnerable to severe epidemic fluctuations [9]. These circumstances highlight the urgent need for robust mathematical models that can explain and predict epidemic dynamics in the Nepalese context.

Traditional epidemiological models such as the SIR, SEIR, and their extensions have played an essential role in understanding infectious disease transmission [6, 21]. They segment the population into compartments based on disease status and use systems of ordinary differential equations to describe transitions between these compartments. Despite their usefulness, classical integer-order models often

fail to adequately represent the memory effects and long-range dependencies that characterize real-world epidemics. COVID-19 transmission, for instance, is strongly influenced by behavioral changes, delayed testing and reporting, vaccination uptake, and the waning of both natural and vaccine-induced immunity[1, 7]. These dynamics cannot be fully captured by models that assume instantaneous transitions between compartments.

Fractional calculus offers an elegant mathematical framework to address this limitation[1]. By extending differentiation and integration to non-integer orders, fractional differential equations naturally incorporate memory and hereditary properties into dynamical systems [17]. In recent years, fractional-order epidemiological models have gained prominence due to their superior ability to fit real epidemic data and reproduce long-term dynamics compared to their integer-order counterparts[15, 16]. For COVID-19 in particular, fractional-order models have demonstrated improved accuracy in describing case trajectories, accounting for non-exponential infection processes, and capturing the effects of delayed or persistent interventions [14].

This study contributes to both the theoretical literature on fractional-order epidemiological models and the applied study of COVID-19 in Nepal. From a theoretical standpoint, the model extends the growing body of fractional epidemic frameworks by incorporating both vaccination and diagnosis compartments. From a practical perspective, it offers valuable insights into the potential outcomes of different control strategies in Nepal, providing guidance for policymakers and public health planners. Ultimately, the integration of fractional calculus with context-specific epidemiological modeling deepens our understanding of COVID-19 transmission dynamics and strengthens the foundation for more effective pandemic preparedness in low- and middle-income countries.

Present study is organized as follows. Section 2 presents the fundamental mathematical definitions and the formulation of the proposed fractional-order epidemic model in Section 3. The positivity and boundedness of solutions are established to ensure biological feasibility in Section 4. Section 5, detailed the stability analysis which is carried out by including the determination of equilibrium points, derivation of the basic reproduction number, investigation of the existence of the endemic equilibrium, and examination of local asymptotic stability conditions. A suitable numerical scheme based on the fractional Euler method is then introduced for solving the system in Section 6. In Section 7, model fitting and parameter estimation techniques are applied using available data to validate the model. Finally, in Section 8, numerical simulations are discussed to illustrate the dynamical behavior of the system, followed by concluding remarks summarizing the main findings.

2 Mathematical definitions

Definition 2.1. [18] The Riemann−Liouville's fractional integral of order η is defined by

$$I_t^{\eta} f(t) = \frac{1}{\Gamma(\eta)} \int_0^t \frac{f(s)ds}{(t-s)^{1-\eta}}$$

where $\eta > 0, t > 0, \Gamma(\eta)$ is gamma function of η

Definition 2.2. [18] The Caputo's fractional derivative of the function $f(t)$ is defined by

$$D_t^{\eta} f(t) = I_t^{n-\eta}[f^n(t)] = \frac{1}{\Gamma(n-\eta)} \int_0^t \frac{D^n f(s)ds}{(t-s)^{\eta-n+1}}, \qquad \text{if } n-1 < \eta < n$$

Definition 2.3. [18] The Laplace transform for the Caputo's fractional derivative of the function f(t) is

$$\mathscr{L}[D_t^{\eta} f(t)] = s^{\eta} F(s) - \sum_{k=0}^{n-1} s^{n-k-1} f^{(k)}(0), \quad n \in \mathbb{N}, \quad n-1 < \eta < n \tag{1}$$

3 Model formulation

The proposed set of equations outlines a fractional-order compartmental model for COVID-19, integrating vaccination, decreasing immunity, and death generated by the disease. This approach includes Caputo fractional derivatives (${}^{C}D_t^{\eta}$) of order η, in contrast to conventional integer-order models, facilitating memory effects in disease transmission dynamics. The population is categorized into six compartments: Susceptible (S), Vaccinated (V), Exposed (E), Infectious (I), Death (D), and Recovered (R).
The Susceptible (S) equation accounts for new births (with a fraction α vaccinated at birth), natural deaths, infection by contact with infected ($\beta SI/N$), vaccination uptake (ϕS), and reinfection owing to fading immunity ($\delta_3 R$). The vaccinated (V) class contains those who got the vaccination yet remain at reduced risk of disease ($\sigma\beta VI/N$, where σ measures vaccine efficacy loss). The exposed (E) group grows through new infections from both susceptible and vaccinated individuals and reduces as latent infections progress to active cases ($\delta_1 E$). The infectious (I) compartment grows via symptom onset and reduces due to recovery ($\delta_2 I$), natural death, and COVID-19 fatalities ($\delta_4 I$). The Death (D) class accumulates deaths from infection, while the Recovered (R) population grows with recoveries but diminishes due to natural mortality and immunity loss ($\delta_3 R$). This model COVID-19 transmission and control techniques. The use of fractional derivatives promotes flexibility in modeling varied disease propagation patterns observed in pandemics [13]. The classical model was discussed by Korolev [8] and the modified fractional-order SVEIDR model is described by the following system of equations:

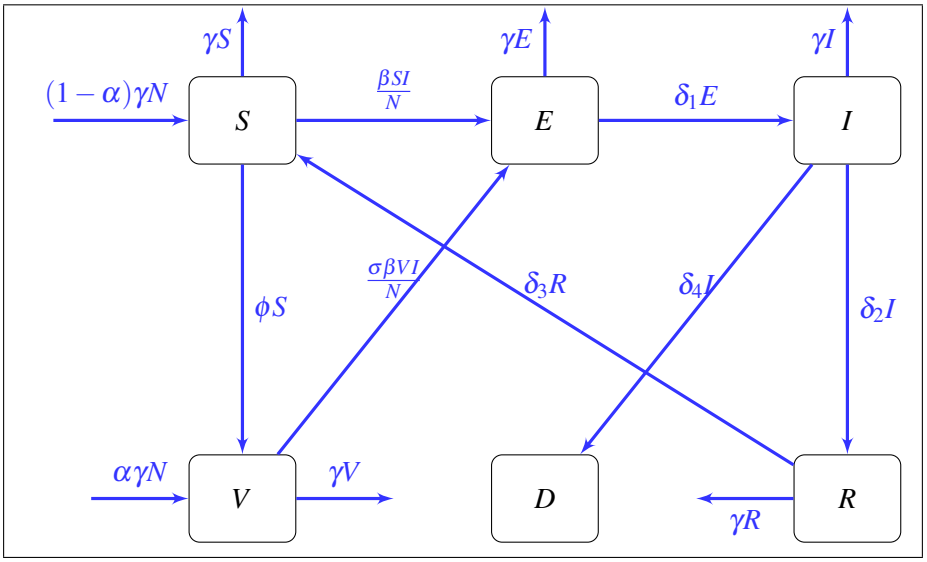

Figure 1: Flow diagram of compartmental model.

$$
\begin{aligned}
{}^{C}D_t^{\eta} S(t) &= (1-\alpha)\gamma N - \gamma S - \frac{\beta SI}{N} - \phi S + \delta_3 R,\\
{}^{C}D_t^{\eta} V(t) &= \alpha\gamma N + \phi S - \frac{\sigma\beta VI}{N} - \gamma V,\\
{}^{C}D_t^{\eta} E(t) &= \frac{\beta SI}{N} + \frac{\sigma\beta VI}{N} - (\delta_1+\gamma)E,\\
{}^{C}D_t^{\eta} I(t) &= \delta_1 E - (\gamma+\delta_2+\delta_4)I,\\
{}^{C}D_t^{\eta} D(t) &= \delta_4 I,\\
{}^{C}D_t^{\eta} R(t) &= \delta_2 I - (\delta_3+\gamma)R.
\end{aligned}
\tag{2}
$$

Initial conditions

Initial conditions for each compartment are, $S(0) > 0, \quad V(0) \geq 0, \quad E(0) \geq 0, \quad I(0) \geq 0, \quad D(0) \geq 0, \quad R(0) \geq 0$. To simplify the notation, let us consider the variables, S, V, E, I, D, R as the fraction of constant population N. Following dynamic equation can be considered in the region $\mathbb{R}^6_+$, such that the dynamics of the system of equations (4) can be studied within $\mathscr{G}$.

$$\mathscr{G} = \{(S,\, V,\, E,\, I,\, D,\, R) \in \mathbb{R}^6_+ : 0 \leq S+V+E+I+D+R \leq 1\} \tag{3}$$

So, we can redefined the model as;

$$\begin{aligned}
{}^{C}D_t^{\eta} S(t) &= (1-\alpha)\gamma - \gamma S - \beta SI - \phi S + \delta_3 R, \\
{}^{C}D_t^{\eta} V(t) &= \alpha\gamma + \phi S - \sigma\beta VI - \gamma V, \\
{}^{C}D_t^{\eta} E(t) &= \beta SI + \sigma\beta VI - (\delta_1 + \gamma)E, \\
{}^{C}D_t^{\eta} I(t) &= \delta_1 E - (\gamma + \delta_2 + \delta_4)I, \\
{}^{C}D_t^{\eta} D(t) &= \delta_4 I, \\
{}^{C}D_t^{\eta} R(t) &= \delta_2 I - (\delta_3 + \gamma)R,
\end{aligned} \tag{4}$$

This fractional-order model captures the memory-dependent behavior of COVID-19 transmission. The fractional derivative enables a more accurate description of incubation periods, delayed recovery, and immunity loss, which are not effectively handled by classical integer-order models [13]. Unlike classical models with integer-order derivatives, fractional-order models (using Caputo's derivatives) incorporate memory effect of the system, i.e. the Caputo's derivative incorporates the entire history of the system, making it suitable for modeling processes with, long-term dependencies (e.g., immune memory) and anomalous diffusion (e.g., disease spread with delays). The current infection rate may depend not only on the present state but also on past states.

4 Non-negative and boundedness

To show non-negativity and boundedness of the given fractional-order epidemiological model using the Caputo's fractional derivative is analyzed for each compartment: $S(t), V(t), E(t), I(t), D(t), R(t)$.

Non-negativity

We assume that initial values for non-negative is as:

$$S(0) \geq 0, \quad V(0) \geq 0, \quad E(0) \geq 0, \quad I(0) \geq 0, \quad R(0) \geq 0, \quad D(0) \geq 0.$$

Using the Caputo's derivative and positivity principle, for the Caputo's derivative ${}^{C}D_t^{\eta} x(t)$, if $x(0) \geq 0$, and $f(x,t) \geq 0$ when $x(t) = 0$, then $x(t) \geq 0$ for all $t > 0$. One verifies that for each compartment, if it reaches zero, then the right-hand side (RHS) is non-negative.

- For $S(t)$, at $S = 0$; ${}^{C}D_t^{\eta} S = (1-\alpha)\gamma + \delta_3 R \geq 0 \Rightarrow S(t) > 0$.
- For $V(t)$, at $V = 0$; ${}^{C}D_t^{\eta} V = \alpha\gamma + \phi S \geq 0 \Rightarrow V(t) \geq 0$.
- For $E(t)$, at $E = 0$; ${}^{C}D_t^{\eta} E = \beta SI + \sigma\beta VI \geq 0 \Rightarrow E(t) \geq 0$.
- For $I(t)$, at $I = 0$: ${}^{C}D_t^{\eta} I = \delta_1 E \geq 0 \Rightarrow I(t) \geq 0$.

- For $D(t)$, at $D=0$, since $I \geq 0$: ${}^{C}D_t^{\eta} D = \delta_4 I \geq 0 \Rightarrow D(t) \geq 0$.
- For $R(t)$, at $R=0$: ${}^{C}D_t^{\eta} R = \delta_2 I \geq 0 \Rightarrow R(t) \geq 0$.

Hence, all compartments remain non-negative for all $t \geq 0$ [19], given non-negative initial conditions.

Boundedness

Let's examine the total living population $N(t) = S(t) + V(t) + E(t) + I(t) + R(t)$ Now, differentiate using Caputo derivative:

$$ {}^{C}D_t^{\eta} N(t) = {}^{C}D_t^{\eta} S + {}^{C}D_t^{\eta} V + {}^{C}D_t^{\eta} E + {}^{C}D_t^{\eta} I + {}^{C}D_t^{\eta} R $$

Substitute from the model:

$$\begin{aligned} {}^{C}D_t^{\eta} N(t) = {} & (1-\alpha)\gamma - \gamma S - \beta SI - \phi S + \delta_3 R \\ & + \alpha\gamma + \phi S - \sigma\beta VI - \gamma V + \beta SI + \sigma\beta VI - (\delta_1 + \gamma)E \\ & + \delta_1 E - (\gamma + \delta_2 + \delta_4)I + \delta_2 I - (\delta_3 + \gamma)R \end{aligned}$$

Since the terms like βSI, $\sigma\beta VI$, and ϕS are cancelled and ombined all terms. We get

$$ {}^{C}D_t^{\eta} N(t) = \gamma - \gamma(S + V + E + I + R) - \delta_4 I = \gamma - \gamma N(t) - \delta_4 I. $$

So, we get ${}^{C}D_t^{\eta} N(t) = \gamma(1 - N(t)) - \delta_4 I(t)$.
Finally, we show that, when $N(t) > 1$, derivative becomes negative implies that $N(t)$ decreases and when $N(t) < 1$, derivative becomes positive implies that $N(t)$ increases. Hence, $N(t)$ is bounded above by N, the total population, and the system tends to keep it around that value. Thus, each compartment is also bounded.

5 Stability analysis

5.1 Equilibrium points

In an epidemic model, an equilibrium point (or steady state) refers to a condition where the number of individuals in each compartments remains constant over time. That is, all derivatives are zero. Disease-Free Equilibrium (DFE), the state where no disease is present i.e $I = 0$ and Endemic Equilibrium (EE), the disease persists in the population at a constant level i.e $I > 0$. In equilibrium state

$$ {}^{C}D_t^{\eta} S = {}^{C}D_t^{\eta} V = {}^{C}D_t^{\eta} E = {}^{C}D_t^{\eta} I = {}^{C}D_t^{\eta} R = {}^{C}D_t^{\eta} D = 0 $$

After solving, we get disease-free equilibrium point as,

$$ Q_0 = (S^0,\, V^0,\, E^0,\, I^0,\, R^0,\, D^0) = \left(\frac{\gamma(1-\alpha)}{\gamma+\phi},\, \frac{\gamma\alpha+\phi}{\gamma+\phi},\, 0,\, 0,\, 0,\, 0 \right) $$

and without vaccination $P_0 = (S^0,\, E^0,\, I^0,\, R^0,\, D^0) = (1,\, 0,\, 0,\, 0,\, 0)$. For the endemic equilibrium point;

$$\begin{aligned} S^* &= \frac{(1-\alpha)\gamma + \delta_3 R}{\gamma + \beta I + \phi}, \quad V^* = \frac{\alpha\gamma N + \phi S}{\sigma\beta I + \gamma}, E^* = \frac{(\gamma+\delta_2)I}{\delta_1}, \\ I^* &= \frac{\delta_1 E}{\gamma + \delta_2 + \delta_4}, \qquad\qquad R^* = \frac{\delta_2 I}{\delta_3 + \gamma}, D^* = 0. \end{aligned} \tag{5}$$

5.2 Basic reproduction number

The basic reproduction number, often denoted as R_0, is a key metric in epidemiology that measures the transmission potential of a disease. It represents the average number of new infections generated by a single infected person in a completely susceptible population [5]. R_0 is not a fixed biological constant for a pathogen. It is a dimensionless number that depends on several factors, including the infectious period of the disease, the contact rate within the population, and the mode of transmission. Since it's an idealized value based on a completely susceptible population, it is often estimated through complex mathematical models [3].

Without vaccination

The disease free equilibrium state P_0 occurs when there is no cases of COVID-19 in the population ($E = I = D = R = 0$). For this, we find the matrices F (infection new cases term) and V (transition terms) of model equations. The Jacobian matrices for F and V are computed and evaluated at P_0 as,

$$F = \begin{bmatrix} 0 & \beta S \\ 0 & 0 \end{bmatrix}, V = \begin{bmatrix} \delta_1 + \gamma & 0 \\ -\delta_1 & \gamma + \delta_2 + \delta_4 \end{bmatrix}.$$

Now, the next generation matrix (FV^{-1}) is determined as,

$$FV^{-1} = \begin{bmatrix} \frac{\delta_1 \beta}{(\gamma+\delta_2+\delta_4)(\delta_1+\gamma)} & \frac{\beta}{\gamma+\delta_2} \\ 0 & 0 \end{bmatrix}.$$

In order to find the spectral radius, eigenvalues λ of the next generation matrix are computed using the following conditions;

$$|FV^{-1} - \lambda I| = 0, \text{ or, } \begin{vmatrix} \frac{\delta_1 \beta}{(\gamma+\delta_2+\delta_4)(\delta_1+\gamma)} - \lambda & \frac{\beta}{\gamma+\delta_2} \\ 0 & 0 - \lambda \end{vmatrix} = 0$$

$$\text{or, } \left(\frac{\delta_1 \beta}{(\gamma + \delta_2 + \delta_4)(\delta_1 + \gamma)} - \lambda \right) (0 - \lambda) = 0$$

Then $\lambda_1 = 0$ and $\lambda_2 = \dfrac{\delta_1 \beta}{(\gamma + \delta_2 + \delta_4)(\delta_1 + \gamma)}$ are the eigenvalues. Since, spectral radius is the largest absolute eigenvalues of the matrix, $\rho(FV^{-1}) = \frac{\delta_1 \beta}{(\gamma+\delta_2+\delta_4)(\delta_1+\gamma)}$. So,

$$R_0 = \frac{\delta_1 \beta}{(\gamma + \delta_2 + \delta_4)(\delta_1 + \gamma)}$$

Here, R_0 represents the basic reproduction number of without vaccination model.

With vaccination

The disease free equilibrium point Q_0 where there are no cases of COVID-19 in the population ($E = I = R = D = 0$). Then, Jacobian matrices F and V are further computed as

$$F = \begin{bmatrix} 0 & \beta S_0 + \sigma \beta V_0 \\ 0 & 0 \end{bmatrix}, V = \begin{bmatrix} \delta_1 + \gamma & 0 \\ -\delta_1 & \gamma + \delta_2 + \delta_4 \end{bmatrix}$$

Now, the eigenvalues of the matrix are determined under the following conditions where λ represents the eigenvalues.

$$|FV^{-1}-\lambda I|=0, \text{ or, } \begin{vmatrix} \frac{\delta_1\beta(S_0+\sigma V_0)}{(\gamma+\delta_2+\delta_4)(\delta_1+\gamma)}-\lambda & \frac{\beta(S_0+\sigma V_0)}{\gamma+\delta_2+\delta_4} \\ 0 & 0-\lambda \end{vmatrix}=0$$

$$\text{or, } \left(\frac{\delta_1\beta(S_0+\sigma V_0)}{(\gamma+\delta_2+\delta_4)(\delta_1+\gamma)}-\lambda\right)(0-\lambda)=0.$$

We obtain $\lambda_1=0$ and $\lambda_2=\dfrac{\delta_1\beta(S_0+\sigma V_0)}{(\gamma+\delta_2+\delta_4)(\delta_1+\gamma)}$. So, the spectral radius is

$$\rho(FV^{-1})=\frac{\delta_1\beta(S_0+\sigma V_0)}{(\gamma+\delta_2+\delta_4)(\delta_1+\gamma)}.$$

$$\begin{aligned} R_{vac} &= \frac{\delta_1\beta(S_0+\sigma V_0)}{(\gamma+\delta_2+\delta_4)(\delta_1+\gamma)}=\frac{\delta_1\beta}{(\gamma+\delta_2+\delta_4)(\delta_1+\gamma)}\cdot\frac{\gamma(1-\alpha)+\sigma(\gamma\alpha+\phi)}{\gamma+\phi} \\ &= R_0\,\frac{\gamma(1-\alpha)+\sigma(\gamma\alpha+\phi)}{\gamma+\phi}. \end{aligned}$$

5.3 Local asymptotically stability

In this section, the study shows that, whether a disease will die out or persist when the system is slightly perturbed around an equilibrium point. Let $X=[S,V,E,I,R]^T$ and the system is linearized near the DFE using the Jacobian matrix has the form:

$$J(Q_0)=\begin{bmatrix} -\gamma-\phi & 0 & 0 & -\beta S^0 & \delta_3 \\ \phi & -\gamma & 0 & -\sigma\beta V^0 & 0 \\ 0 & 0 & -(\delta_1+\gamma) & \beta S^0+\sigma\beta V^0 & 0 \\ 0 & 0 & \delta_1 & -(\gamma+\delta_2+\delta_4) & 0 \\ 0 & 0 & 0 & \delta_2 & -(\delta_3+\gamma) \end{bmatrix}$$

Which implies that,

$$(\lambda+\gamma+\phi)(\lambda+\gamma)(\lambda+\delta_3+\gamma)\left[(\lambda+\delta_1+\gamma)(\lambda+\gamma+\delta_2+\delta_4)-\delta_1\cdot\frac{\beta\gamma(1-\alpha)+\sigma\beta(\gamma\alpha+\phi)}{(\gamma+\phi)}\right]=0$$

The terms $(\lambda+\gamma+\phi),\quad(\lambda+\gamma),\quad(\lambda+\delta_3+\gamma)$ correspond to the eigenvalues from the non-infectious compartments: S, V, and R. The bracketed expression involves the infected subsystem and determines local stability of the disease-free equilibrium. Its form resembles a quadratic in λ and is key to defining the basic reproduction number R_0. For a Caputo fractional-order system of order $\eta\in(0,1]$, the DFE is locally asymptotically stable if and only if all eigenvalues λ_i of the Jacobian matrix satisfy [11]:

$$|\arg(\lambda_i)|>\frac{\eta\pi}{2},\quad\forall i.$$

The eigenvalues from the first three terms are as; $\lambda_1=-(\gamma+\phi),\quad\lambda_2=-\gamma,\quad\lambda_3=-(\delta_3+\gamma)$. All of these are real and negative, so they satisfy: $|\arg(\lambda_i)|=\pi>\frac{\eta\pi}{2}\quad$ for all $\eta\in(0,1]$. The remaining two eigenvalues come from the roots of the quadratic equation:

$$(\lambda+\delta_1+\gamma)(\lambda+\gamma+\delta_2+\delta_4)=\delta_1\cdot\frac{\beta\gamma(1-\alpha)+\sigma\beta(\gamma\alpha+\phi)}{(\gamma+\phi)}$$

$$\mathscr{K}=\delta_1\cdot\frac{\beta\gamma(1-\alpha)+\sigma\beta(\gamma\alpha+\phi)}{(\gamma+\phi)}$$

$$\Rightarrow \lambda^2 + A\lambda + B - \mathscr{K} = 0$$

where, $A = 2\gamma + \delta_1 + \delta_2 + \delta_4, \quad B = (\delta_1 + \gamma)(\delta_2 + \delta_4 + \gamma)$. Thus, the eigenvalues are:

$$\lambda_{4,5} = \frac{-A \pm \sqrt{A^2 - 4(B - \mathscr{K})}}{2}$$

Since, all parameters are positive, if $\mathscr{K} < B$, then the real parts of both eigenvalues are negative. In this case, the eigenvalues lie in the left-half complex plane, and the angle condition, $|\arg(\lambda_i)| > \frac{\eta\pi}{2}$ is automatically satisfied for all $\eta \in (0, 1]$, ensuring local asymptotic stability. For the Caputo fractional-order system of order $\eta \in (0, 1]$, the disease-free equilibrium is locally asymptotically stable if

$$\delta_1 \cdot \frac{\beta\gamma(1-\alpha) + \sigma\beta(\gamma\alpha + \phi)}{(\gamma + \phi)} < (\delta_1 + \gamma)(\delta_2 + \delta_4 + \gamma).$$

which implies that $R_{vacc} < 1$. In this case, all eigenvalues λ_i of the Jacobian satisfy the condition $|\arg(\lambda_i)| > \frac{\eta\pi}{2}, \quad \forall i$, which guarantees local asymptotically stability of the disease-free equilibrium.

5.4 Existence of endemic equilibrium

The simplification of the system of equations (4) leads to another equilibrium, known as endemic equilibrium points which are denoted as $Q^* = (S^*, V^*, E^*, I^*, R^*)$. We further investigate the existence of endemic equilibrium in the model. For which, the following are the conditions for any equilibrium point. Using E^* in exposed compartment, we get

$$\begin{aligned} E^* &= \frac{(\gamma + \delta_2)I}{\delta_1} \\ \text{and , } \beta SI + \sigma\beta VI - (\delta_1 + \gamma)\frac{(\gamma + \delta_2)I}{\delta_1} &= 0 \\ \text{or, } \beta SI\delta_1 + \sigma\beta VI\delta_1 - (\delta_1 + \gamma)(\gamma + \delta_2)I &= 0 \\ \text{or, } \beta\delta_1(S + \sigma V) &= (\delta_1 + \gamma)(\gamma + \delta_2). \end{aligned}$$

Since $(S + \sigma V) < 1$, this equation can be true only for $\beta\delta_1 > (\delta_1 + \gamma)(\gamma + \delta_2)$; hence, there exists no endemic equilibrium for $R_0 \leq 1$.

6 Numerical scheme

The fractional Euler's method is a numerical approach used to solve fractional differential equations (FDEs). Unlike classical ordinary differential equations (ODEs), FDEs involve derivatives of non-integer order (e.g., Caputo or Riemann-Liouville fractional derivatives), making their analytical and numerical treatment more complex. The memory dependence is unlike the classical Euler method, fractional Euler incorporates past values due to the non-local nature of fractional derivatives [10]. The convergence of the method has an error bound of $O(h^\eta)$ for $0 < \eta < 1$[20].

Algorithm steps

1. Initialize y_0 and $t_0 = 0$.
2. For $n = 0$ to $N - 1$:

- Compute $f_n = f(t_n, y_n)$.
- Update the solution using the weighted sum: $y_{n+1} = y_0 + \frac{h^\eta}{\Gamma(\eta+1)} \sum_{j=0}^{n} w_{j,n} f_j$ where, $w_{j,n} = (n+1-j)^\eta - (n-j)^\eta$.

3. Return the solution $\{y_n\}$ at each time step.

7 Model fitting and parameter estimations

The model 4 is fitted using the least square method on data of COVID-19 cases in Nepal as recorded by MOHP [12]. In Figure (2a), the red-circled bubbles represent the active infected cases of the COVID-19 patients in Nepal prevailing from mid of September, 2021 to beginning of February, 2022. While the solid blue line represents the estimated cases of the COVID-19 using the model (4). The fitted model well cooperates the nature of the infected cases of COVID-19 in real world scenario. Figure (2a) illustrates a comparison between the real cumulative COVID-19 case data and the corresponding model-fitted curve over time. The horizontal axis represents time, starting from the initial outbreak and extending to about 140 days, while the vertical axis shows the cumulative number of reported cases, ranging from approximately 50,000 to 300,000. Fitted model curve not only validates the model's accuracy but also helps in predicting future trends and assessing the impact of control measures.

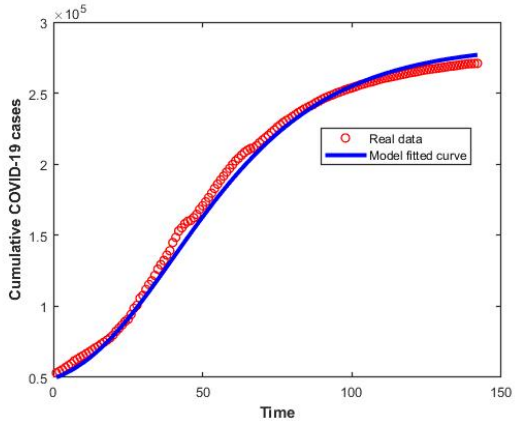

(a) Model parameters prediction using cumulative COVID-19 data.

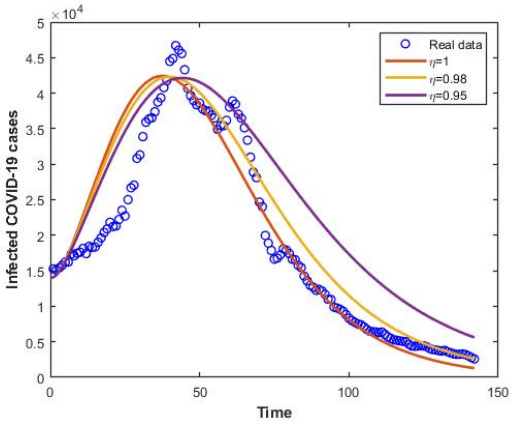

(b) Model validation with fractional order derivative model at $\eta = 0.98$.

Figure (2b) compares real daily infected COVID-19 case data with model simulations for different values of the fractional order η. The horizontal axis represents time in days, while the vertical axis shows the number of infected cases, ranging from zero to about 50,000. The three solid curves correspond to model predictions for fractional orders $\eta = 1$, $\eta = 0.98$, and $\eta = 0.95$. The case $\eta = 1$ represents the classical integer-order model and matches the real data most closely, capturing both the peak height and timing as well as the decline rate. In contrast, the fractional-order models ($\eta < 1$) show a slower decay after the peak, producing a longer epidemic tail and slightly delayed peak times. This behavior reflects the memory and non-local effects in fractional-order model, where past states influence current dynamics more strongly, leading to a more prolonged epidemic spread. The comparison demonstrates that adjusting the fractional order provides flexibility in capturing complex epidemic patterns beyond what the integer-order model offers.

The parameters as described in the model (4) are estimated and predicted in order to establish a suitable match between reported and predicted infected cases of COVID-19 in Nepal from mid of September, 2021

to first of February, 2022 [12]. The total population is assumed as $N = 2 \times 10^7$. The initial vaccinated human population is $V_{h0} = 2{,}000$, the exposed human population is $E_{h0} = 35{,}000$, and the infected human population is $I_{vh0} = 14{,}000$. Additionally, the initial recovered population is $R_{v0} = 20{,}000$. These values are according to the current situations. The parameter γ is assumed as $\frac{1}{70 \times 365}$ per day [2]. The estimated parameter values are listed in Table 1.

Parameters	α	σ	ϕ	β	δ_1	δ_2	δ_3	δ_4
Values	0.01	0.05	0.04	0.5209	0.05	0.09	0.02	0.025
References	Assumed	Assumed	Assumed	Fitted	Fitted	Fitted	Fitted	Assumed

Table 1: The estimated parameters value.

8 Numerical discussions

In this section, the numerical results on basic reproduction number and graphical representation on fractional-order derivative is presented.

8.1 Simulation of basic reproduction number

Figure (3a) shows the variation of the vaccination reproduction number R_{vac} as a function of the parameters α (vaccine efficacy loss rate) and ϕ (vaccination rate). The surface indicates that R_{vac} increases slightly with higher α when ϕ is small, while higher ϕ tends to reduce R_{vac}, reflecting the impact of increased vaccination coverage in lowering disease spread. The effect of α is more pronounced at very low ϕ, where a steep gradient appears. Figure (3b) shows R_{vac} as a function of σ (reduction in susceptibility for vaccinated individuals) and ϕ. Here, R_{vac} decreases sharply with higher ϕ, regardless of σ, illustrating that increasing vaccination rate is a dominant factor in reducing transmission. Additionally, higher σ

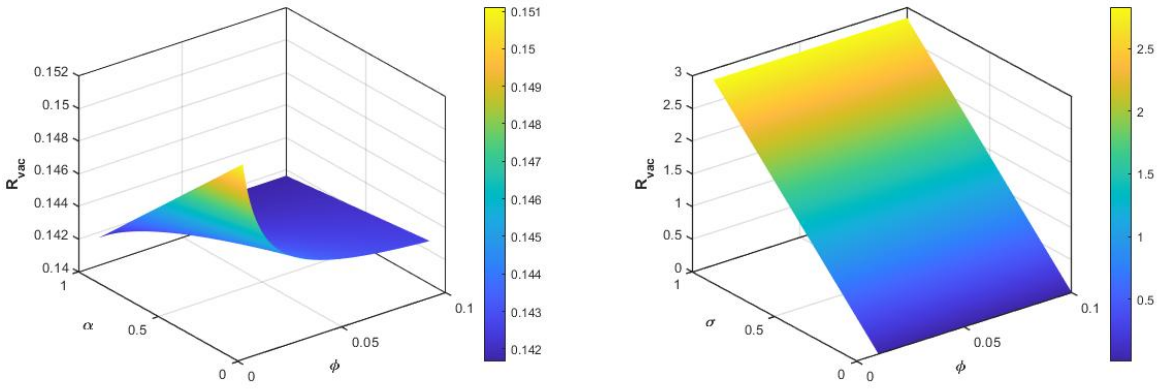

(a) Relation between R_{vac}, α, and ϕ

(b) Relation between R_{vac}, ϕ, and σ

Figure 3: Relation between R_{vacc} on different parameters

increases R_{vac}, indicating that reduced protection in vaccinated individuals leads to greater transmission potential, but this effect diminishes when ϕ is large. Together, these plots highlight how the interplay between vaccination rate and vaccine-related parameters shapes the potential for disease spread under vaccination strategies. Figure (3b) shows R_{vac} as a function of σ (reduction in susceptibility for vaccinated

individuals) and ϕ. Here, R_{vac} decreases sharply with higher ϕ, regardless of σ, illustrating that increasing vaccination rate is a dominant factor in reducing transmission. Additionally, higher σ increases R_{vac}, indicating that reduced protection in vaccinated individuals leads to greater transmission potential, but this effect diminishes when ϕ is large. Together, these plots highlight how the interplay between vaccination rate and vaccine-related parameters shapes the potential for disease spread under vaccination strategies.

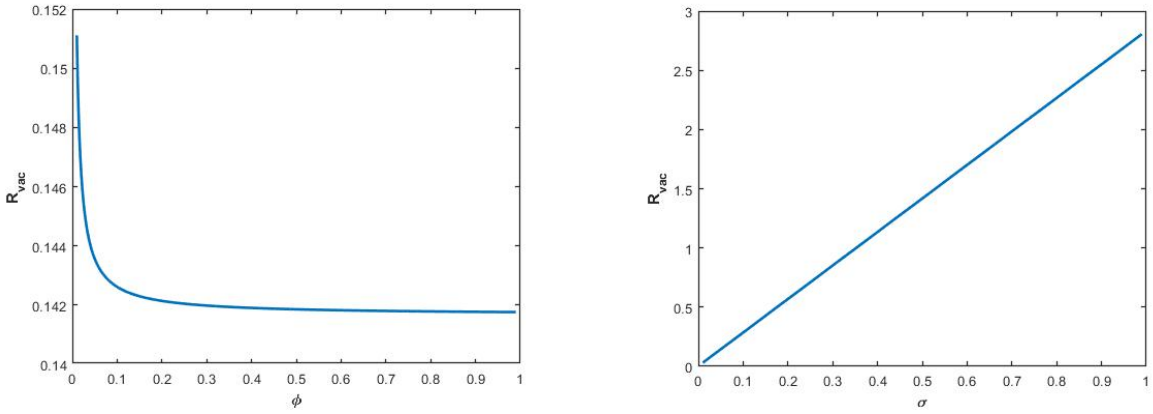

(a) Relation between $R_{vac}$and ϕ (b) Relation between $R_{vac}$and σ

Figure 4: Graphical relation of R_{vacc} on different parameters

This Figures ((4a) and (4b)) presents the relationship between the vaccination reproduction number R_{vac} and the vaccination rate ϕ, while keeping other parameters fixed. The curve exhibits a steep negative slope for very small values of ϕ, indicating that even a small increase in vaccination coverage at low levels leads to a significant reduction in R_{vac}. As ϕ increases further, the curve begins to flatten out, approaching a lower asymptotic value near $R_{\text{vac}} \approx 0.142$. This behavior implies diminishing returns, once a certain level of vaccination coverage is achieved, additional increases in ϕ only yield marginal improvements in reducing R_{vac}. The biological interpretation is that, beyond a certain point, most susceptible individuals are already protected, and the disease transmission potential becomes limited by other factors such as partial immunity, waning protection, or non-vaccinated pockets in the population. This pattern is typical in epidemiological modeling, highlighting the critical importance of rapid initial vaccination deployment to achieve effective control over an outbreak.

8.2 Graphical results of model equations

Figures (5) depict the dynamics of a COVID-19 disease over time, likely modeled using a fractional order derivative compartmental epidemiological model. Each subplot shows how a specific population group changes over time, with three different curves corresponding to varying values of a parameter denoted by 'η'. The parameter 'η' appears to represent the effectiveness or rate of vaccination, with values of one (blue), 0.98 (red), and 0.95 (yellow), where a higher value signifies a more effective or faster vaccination process. The susceptible population decreases over time, with the most rapid decline observed when vaccination effectiveness is highest ($\eta = 1$), compared to $\eta = 0.98$ and $\eta = 0.95$. This trend reflects the fact that stronger vaccination coverage transfers more individuals from the susceptible class to the vaccinated class at a faster rate. The plot in the top-right, "Vaccination population," confirms this by showing an increase in the vaccinated population over time. The rate of this increase is highest for $\eta = 1$, leading to a higher final vaccination count, and progressively lower for $\eta = 0.98$ and $\eta = 0.95$, directly reflecting the assumed effectiveness of the vaccination. The exposed and infected compartments follow

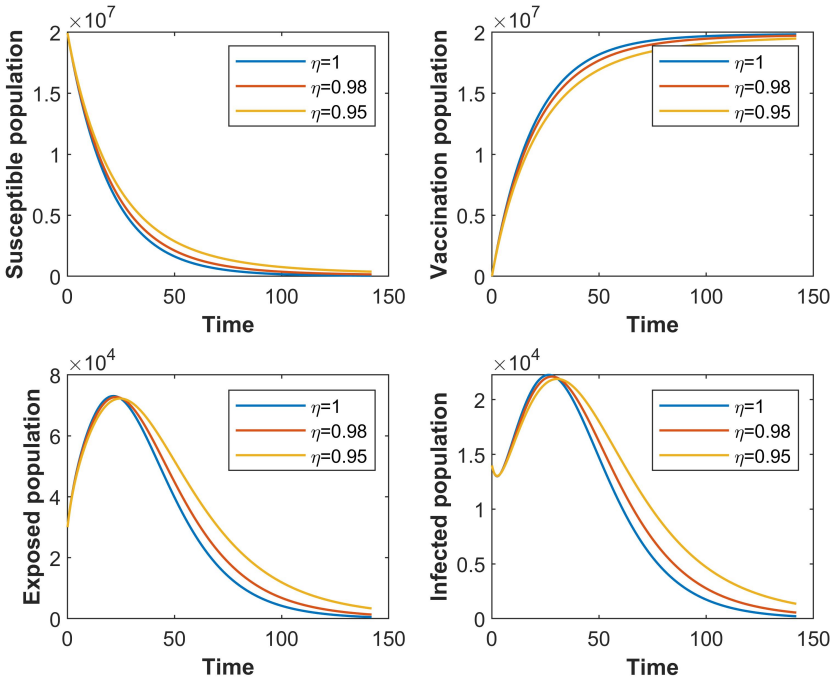

Figure 5: Fractional order derivative impact on different compartments.

a typical epidemic wave, where cases rise and later decline. Under $\eta = 1$, peaks occur earlier and at a lower magnitude than with $\eta = 0.98$ and $\eta = 0.95$. This shows that stronger vaccination effectiveness not only reduces the number of cases but also shortens the outbreak duration.

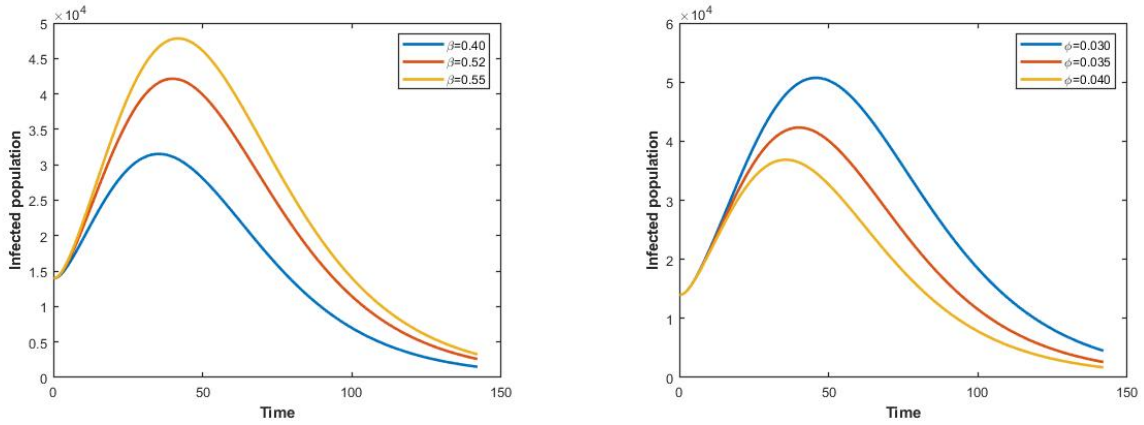

(a) Effects of β on infected population at $\eta = 0.98$.

(b) Effects of ϕ on infected population at $\eta = 0.98$.

Figure 6: Effects of parameters on infected population at $\eta = 0.98$.

Figures ((6a) and (6b)) illustrate the dynamics of an Infected population over time, likely as part of an epidemiological model. Each plot shows how the number of infected individuals changes in response to variations in a specific parameter, while other parameters are held constant. Figure (6a) illustrates that higher transmission rates (β) amplify epidemic severity. As β increases, the infection curve peaks later and at higher levels, implying that reducing contact or transmission probability is crucial for epidemic mitigation. Therefore, to control the spread of the disease, efforts would need to focus on reducing the

value of the parameter β. In Figure (6b), changes in the vaccination rate parameter ϕ alter the infection curve. Increasing ϕ shifts the epidemic peak downward and forward in time, indicating that higher vaccination coverage accelerates control of the outbreak.

9 Conclusion

In this study, the Caputo's fractional-order model for the COVID-19 epidemic in Nepal, that includes vaccination. The study focuses on the stability and boundedness of the model's disease-free state. Graphical simulations is used to analyze the basic reproduction number and the impact of both vaccination-related parameters and the memory index (η). The fractional Euler's numerical technique is used to generate these visualizations.

By incorporating a fractional derivative (η), the model accounts for "memory effects" and behavioral responses that traditional integer-order models. The findings highlight that early vaccination is highly effective in controlling the spread of the disease, with even a small number of immunized people significantly reducing transmission potential. The biological conclusion is that once a large portion of the susceptible population is protected, disease spread is limited by factors like partial or waning immunity and non-vaccinated groups in Nepal. Further investigation can be undertaken through comprehensive sensitivity analysis and the implementation of rigorous control strategies for the fractional order derivative COVID-19 model.

References

[1] Atangana, A., & Baleanu, D. **(2020)**, New fractional derivatives with nonlocal and non-singular kernel: Theory and application to COVID-19. *Chaos, Solitons & Fractals*, **139**: 110066. https://doi.org/10.1016/j.chaos.2020.110066.

[2] Central Bureau of Statistics Nepal. **(2021)**, *National Population and Housing Census 2021*. https://cbs.gov.np.

[3] Carlos-Chavez, C., Zhilan, F., & Huang, W. **(2002)**, On the computation of R_0 and its role on global stability, *Mathematical Approaches for Emerging and Reemerging Infectious Diseases: An Introduction*, **125**: 229–250, Springer, New York, NY, USA.

[4] Cucinotta, D., & Vanelli, M. **(2020)**, WHO declares COVID-19 a pandemic. *Acta Biomedica*, **91(1)**: 157–160. https://doi.org/10.23750/abm.v91i1.9397.

[5] Driessche, P. van den, & Watmough, J. **(2002)**, Reproduction numbers and sub-threshold endemic equilibria for compartmental models of disease transmission, *Mathematical Biosciences*, **180**: 29–48.

[6] Hethcote, H. W. **(2000)**, The mathematics of infectious diseases. *SIAM Review*, **42(4)**: 599–653. https://doi.org/10.1137/S0036144500371907.

[7] Ke, R., Romero-Severson, E., Sanche, S., & Hengartner, N. **(2021)**, Estimating the reproductive number R_0 of SARS-CoV-2 in the United States and eight European countries and the impact of vaccination and waning immunity. *PLoS Computational Biology*, **17(7)**: e1009235.

[8] Korolev, I. **(2021)**, Identification and estimation of the SEIRD epidemic model for COVID-19. *Journal of Econometrics*, **220**: 63–85.

[9] Kuikel, S., et al. **(2023)**, A critical analysis of health system in Nepal: Perspectives based on COVID-19 response. *Dialogues in Health*, **3**: 100142.

[10] Li, C., & Zeng, F. **(2015)**, *Numerical Methods for Fractional Calculus*, Chapman and Hall/CRC, London, UK.

[11] Matignon, D. **(1996)**, Stability results for fractional differential equations with applications to control processing. *Computation Engineering System and Application*, **2**: 963–968.

[12] Ministry of Health and Population, Nepal, **(2020)**, COVID-19 Dashboard. Retrieved from https://covid19.mohp.gov.np/situation-report.

[13] Omame, A., Nwajeri, U. K., Abbas, M., & Onyenegecha, C. P. **(2022)**, A fractional order control model for diabetes and COVID-19 co-dynamics with Mittag-Leffler function. *Alexandria Engineering Journal*, **61(10)**: 7619–7635. https://doi.org/10.1016/j.aej.2022.01.012.

[14] Owolabi, K. M., & Atangana, A. **(2020)**, Mathematical analysis and computational experiments for fractional epidemiological models: COVID-19 dynamics with memory effect. *Chaos, Solitons & Fractals*, **138**: 109922. https://doi.org/10.1016/j.chaos.2020.109922.

[15] Pandey, H. R., Phaijoo, G. R., & Gurung, D. B. **(2023)**, Analysis of dengue infection transmission dynamics in Nepal using fractional order mathematical modeling. *Chaos, Solitons & Fractals: X*, **11**: 100098. https://doi.org/10.1016/j.csfx.2023.100098.

[16] Pandey, H. R., Phaijoo, G. R., & Gurung, D. B. **(2024)**, Dengue dynamics in Nepal: A Caputo fractional model with optimal control strategies. *Heliyon*, **10(13)**: e33822. https://doi.org/10.1016/j.heliyon.2024.e33822.

[17] Pandey, H. R., Phaijoo, G. R., & Gurung, D. B. **(2024)**, A comprehensive study of fractional-order derivatives and their interplay with basic functions. *Journal of Nepal Mathematical Society*, **6(2)**: 38–52. https://doi.org/10.3126/jnms.v6i2.63023.

[18] Podlubny, I. **(1999)**, *Fractional Differential Equations*, Mathematics in Science and Engineering, Vol. 198, Academic Press, San Diego, CA, USA.

[19] Odibat, Z. M., & Shawagfeh, N. T. **(2007)**, Generalized Taylor's formula. *Applied Mathematics and Computation*, **186**: 286–293.

[20] Odibat, Z. M., & Moamni, S. **(2008)**, An algorithm for the numerical solution of differential equations of fractional order. *Journal of Applied Mathematics and Informatics*, **26**: 15–27.

[21] Kermack, W. O., & McKendrick, A. G. **(1927)**, A contribution to the mathematical theory of epidemics. *Proceedings of the Royal Society A*, **115(772)**: 700–721. https://doi.org/10.1098/rspa.1927.0118.

[22] Wikipedia contributors. **(2025)**, COVID-19 pandemic in Nepal. In Wikipedia. *Retrieved from https://en.wikipedia.org/wiki/COVID-19 pandemic in Nepal*.

□□